City Research Online

City, University of London Institutional Repository

This is the accepted version of the paper.

This version of the publication may differ from the final published version.

Did the Draupner wave occur in a crossing sea?

T.A.A. Adcock[1], P.H. Taylor[1], S. Yan[2], Q.W. Ma[2] and P.A.E.M. Janssen[3]

[1] *Department of Engineering Science, University of Oxford, UK*
[2]*School of Engineering and Mathematical Sciences, City University, London, UK*
[3]*European Centre for Medium-Range Weather Forecasts, Reading, UK*

The 'New Year Wave' was recorded at the Draupner platform in the North Sea and is a rare high quality measurement of a 'freak' or 'rogue' wave. The wave has been the subject of much interest and numerous studies. Despite this, the event has still not been satisfactorily explained. One piece of information which was not directly measured at the platform, but which is vital to understanding the nonlinear dynamics is the wave's directional spreading. This paper investigates the directionality of the Draupner wave and concludes it might have resulted from two wave-groups crossing, whose mean wave directions were separated by about 90° or more.

This result has been deduced from a set-up of the low frequency second order difference waves under the giant wave, which can be explained only if two wave systems are propagating at such an angle. To check whether second order theory is satisfactory for such a highly non-linear event, we have run numerical simulations using a fully non-linear potential flow solver, which confirm the conclusion deduced from the second order theory. This is backed up by a hindcast from ECMWF which shows swell waves propagating at ∼80° to the wind sea. Other evidence which supports our conclusion are the measured forces on the structure, the magnitude of the second order sum waves and some other instances of freak waves occurring in crossing sea states.

Key words: Draupner, New Year Wave, Freak wave, Rogue wave.

1. Introduction

On 1 January 1995 a large wave was recorded at the Draupner platform in the North Sea (Figure 1). This has been variously referred to as the 'Draupner wave' or the 'New Year Wave'. The free surface was recorded with a downward pointing laser sampling at 2.1Hz. The platform, which stands in 70m water-depth, has a sparse structure which would have had a negligible effect on the motion of the wave, and the record is therefore assumed to be an undisturbed field measurement.

The giant wave had a crest 18.6m above mean sea level and was 25.6m in height. Other properties of the individual wave are given in Guedes Soares *et al.* (2004). Despite being very steep, there is no obvious sign in the data that the wave was breaking. The storm properties were approximately stationary over a five hour period, with $H_s = 12$m and $T_z = 12.5$s. The data are not continuous, and were recorded for only 20 minutes in every hour. For more information on the structure, the instrumentation, the meteorological conditions and the wave record,
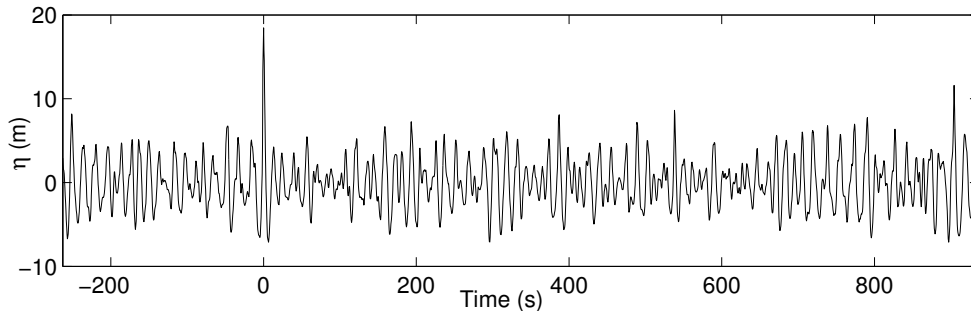
Figure 1. The surface elevation time history recorded at the Draupner platform which includes the New Year Wave. For convenience the time is set to zero under the big wave.

see Haver (2004). Haver discusses at length the presumed nature of the wind and wave fields and observes that minor structural damage to robust equipment below main deck level on the platform was found after the storm. This damage was at an elevation consistent with the size of the large crest which is the subject of this paper. So we may be reasonably confident that green water reached this level and the wave record is reliable. Numerous others have studied the properties of this wave: see for instance Trulsen (2001); Walker *et al.* (2005); Jensen (2005); Clauss & Klein (2009).

The most common explanation given for the Draupner wave is that resonant wave-wave interactions caused a non-linear focusing of wave energy. This focusing has been shown to occur for narrow-banded uni-directional waves in deep water (Janssen, 2003; Onorato *et al.*, 2009). However, these interactions reduce considerably if finite depth and directional spreading are taken into account. The non-dimensional water depth for the Draupner wave was $kd = 1.6$, which is close to the finite depth limit of the narrow banded approximation to the Zakharov equation ($kd = 1.36$) where the Benjamin-Feir Index goes to zero (Onorato *et al.*, 2006a; Janssen & Onorato, 2007). This implies that non-linear wave-wave focusing, as we currently understand it, will be small in this sea-state. Directional spreading also reduces these non-linear interactions (Waseda *et al.*, 2009). The sea-state at Draupner is unlikely to have had a mean directional spreading less than 20° r.m.s. (see section 2). The numerical simulations of Gramstad & Trulsen (2007) and the result reported in Toffoli *et al.* (2010) suggest that with this spreading there will be no extra elevation, even in deep water, over that expected by second order theory.

A number of other explanations have been proposed to explain freak waves (Kharif & Pelinovsky, 2003), which we will briefly consider here. The water depth at Draupner is too deep for the bathymetric steering to be significant and thus ray-focusing may be dismissed as a possible cause. Due to the strong wind, there will have been a wind driven current; these are difficult to quantify accurately, but we can be fairly certain that it would have been going in broadly the same direction as both the wind and the waves and will therefore not increase the chances of a freak wave (Hjelmervik & Trulsen, 2009). The tidal current at the Draupner platform at the time of the giant wave is predicted to be less than 0.2m/s by the Admiralty's Total Tide software, which is too small to induce

significant wave/current interactions. The platform is too far west to be affected by the Norwegian Current. A final possibility, that localised wind/wave interactions might cause a localised increase in wave amplitude, is, at the time of writing, poorly understood.

Whilst a large wave might be caused by the random superposition of linear waves, a wave crest of this magnitude is unlikely in this sea-state. Assuming wave crests follow a Forristall distribution (Forristall, 2000) one would expect a crest of this magnitude only once in more than 3×10^6 waves (third order bound harmonics may reduce this figure slightly (Zheng & Moan, 2010) but the wave remains improbable). No concrete physical explanation for the giant Draupner wave has been found. One aspect of the wave which suggests very strongly that it was in some way abnormal was the low frequency set-up under the giant wave as first observed by Walker *et al.* (2005), whereas typically one observes a set-down under a large wave. This aspect has not been thoroughly explored.

In this paper we try to reconstruct the directional spreading of the Draupner wave, which was not directly measured, but which is vital to understanding the non-linear dynamics of large waves. In doing this we explain the low frequency 'set-up' under the giant wave. We show, both analytically and with numerical simulations, that this only occurs when two wave systems cross at an angle greater than around 90° (see also Toffoli *et al.* (2007); Christou *et al.* (2009)). We find that this is consistent with other evidence including the hindcast of the sea-state from ECMWF and the measured forces on the structure. Finally we consider other freak waves which have occurred in "crossing" sea-states.

2. Spreading of the Draupner sea-state

No directional information was recorded at the Draupner platform. The nearest location known to the authors where directional data for this storm was recorded is the Auk platform 180km away (Ewans, private communication). The meteorological conditions suggest this was part of the same storm, and the other sea-state parameters are similar. At Auk, the directional spreading had a standard deviation about the mean direction of 20° when a weighted average is taken over all frequencies. This measurement is in agreement with the analysis of Adcock & Taylor (2009a) who used the second order bound waves to estimate the directionality of the sea-state over the duration of the storm. It should however be noted that this analysis broke down in the vicinity of the giant wave, this is discussed further in section 4b. Hindcast data from ECMWF suggests a slightly higher spreading of 25° although this was for several hours before the storm reached its maximum intensity.

A more detailed analysis of the ECMWF results show that 3 hours before the giant wave, in addition to the wind sea, there was also a small swell present at the Draupner location. This was in a markedly different direction to the wind sea, as shown in Figure 2. Although this sea-state is timed at 12:00 it should be recalled that the output from a hindcast is of significant waveheight (H_s) averaged over both space and time. So short duration peaks in H_s may be missed. Also Haver (2004) describes the sea-state as arising from a large winter depression and a short duration 'Arctic bomb', a much smaller but more violent wind field with a significantly different mean direction.
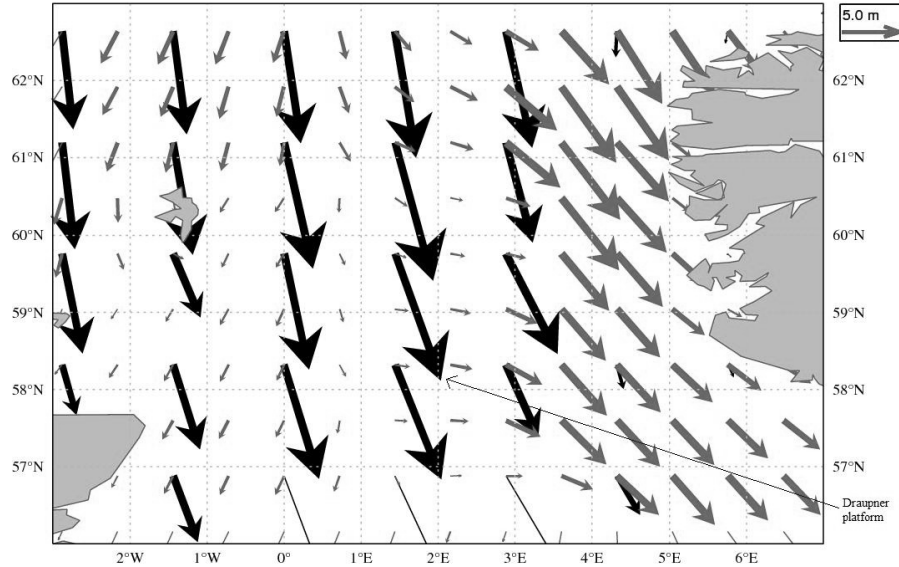
Figure 2. Hindcast of the wave climate in the northern North Sea at 12:00 on January 1 1995. The north coast of Scotland and the Shetland Islands are on the left of the figure with the south-west Norweigan coast on the right. The Draupner platform is located at $58°11'60''$N $2°2'821''$E as indicated. The black arrows represent the wind sea significant wave height, the grey arrows are the swell.

Although the ERA hindcast from ECMWF is produced using more recent version of the WAM model than that described in the book by Komen *et al.* (1994), there must still be some uncertainty in the accuracy of sea-states arising from fast varying local wind fields. In this book Holthuijsen (section II.10) discusses this problem, which may be intrinsic in area and time averaged models. An interesting more recent discussion of at least some of the problems associated with hindcasting sea-states in regions with fast varying winds is given in Jensen *et al.* (2006).

The idea of crossing sea components is consistent with the analysis of SAR images by Rosenthal & Lehner (2008).

3. The spectrum of the Draupner sea-state

The spectrum of the Draupner wave record has been studied in detail by Ewans & Buchner (2008). Here we consider the Fourier energy spectrum around the Draupner wave and show it is significantly different to that of the rest of the storm. Figure 3 shows estimated mean spectra for all six of the hourly 20 minute records available during the storm, the 20 minute record containing the Draupner wave, and a five minute and two minute record centered on the Draupner wave, albeit these last two being rather coarse representations.

 It can be seen that for five minutes of data around the giant wave, the spectrum is similar to that for longer time periods, which in turn are similar in form to a JONSWAP spectrum with a peak at around 0.067Hz. In the 2 minute spectrum
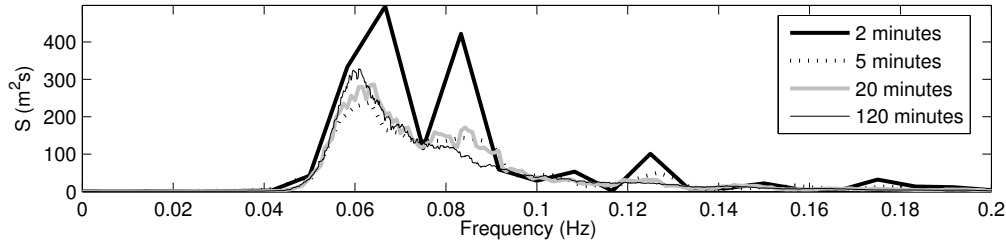
Figure 3. Spectra of time-records containing the Draupner wave. The 2 and 5 minute records are centered on the giant wave. The 20 minute is the spectrum of the data shown in Figure 1. The 120 minute spectrum is based on all the available data for the storm. Data is windowed using a Hann window. The data is smoothed by taking an average over 0.001Hz to improve the clarity of the longer data sets.

there is a clear second peak at 0.083Hz. We call the peak around 0.067Hz – peak 1, and the peak near 0.0833Hz – peak 2.

A broadening of the spectrum due to non-linear wave-wave interactions is known to occur around large waves in deep water. This result is found in experimental studies (Johannessen & Swan, 2001), numerical studies (Gibbs & Taylor, 2005), analytically (Adcock & Taylor, 2009b; Adcock, 2009) and in field data by Krogstad et $al.$ (2006). However this effect is greatly reduced in finite depth (Adcock & Yan, 2010; Katsardi & Swan, 2011). Even if the spectral broadening is due to resonant wave-wave interactions, we would not normally expect these to form a double peak. However, the window used is short and so this may be an artifact of the coarse resolution of the Fourier transform. We will return to this double peak feature in section 4b.

4. Bound waves

Freely propagating, or linear, waves will interact to produce 'bound' waves which do not move independently. To second order, these waves will occur at the sum and difference of the frequencies of the linear waves. The freely propagating waves may be written as

$$\eta_{free} = \sum_{n=1}^{n=N} a_n \cos\left(\phi_n\right), \tag{4.1}$$

where a_n is the Fourier coefficient, N the number of Fourier components used, and

$$\phi_n = \omega_n t + \xi_n, \tag{4.2}$$

where ξ gives the relative phase of the component.

The linear waves in equation 4.1 will interact to give a second order sea state given by

$$\eta = \eta_{free} + \eta_{2+} + \eta_{2-}, \tag{4.3}$$

where

$$\eta_2^{\pm} \;\; = \;\; \sum_{n=1}^{n=N} \sum_{m=1}^{m=N} a_n a_m \kappa^{\pm} \cos\left(\phi_n \pm \phi_m\right), \tag{4.4}$$

where κ^+ and κ^- are the interaction kernels given in equations 4.5. The kernels for finite depth were first given in Dean & Sharma (1981), see also Dalzell (1999) where corrections to the finite depth case are given.

$$\kappa^{\pm} \;\; = \;\; \frac{\omega_n^2 + \omega_m^2}{2g} + \frac{\omega_n \omega_m}{2g} \left(\frac{\cos\theta}{\tanh(|\mathbf{k}_n|\,d)\tanh(|\mathbf{k}_m|\,d)} \mp 1 \right) \times$$

$$\left(\frac{(\omega_n \pm \omega_m)^2 + g\,|\mathbf{k}_n \pm \mathbf{k}_m|\tanh(|\mathbf{k}_n \pm \mathbf{k}_m|\,d)}{(\omega_n \pm \omega_m)^2 - g\,|\mathbf{k}_n \pm \mathbf{k}_m|\tanh(|\mathbf{k}_n \pm \mathbf{k}_m|\,d)} \right) +$$

$$\left(\frac{\omega_n \pm \omega_m}{2g\left((\omega_n \pm \omega_m)^2 - g\,|\mathbf{k}_n \pm \mathbf{k}_m|\tanh(|\mathbf{k}_n \pm \mathbf{k}_m|\,d)\right)} \right) \times$$

$$\left(\frac{\omega_n^3}{\sinh^2(|\mathbf{k}_n|\,d)} \pm \frac{\omega_m^3}{\sinh^2(|\mathbf{k}_m|\,d)} \right). \tag{4.5}$$

The magnitude of the wavenumber $|\mathbf{k}|$ and natural frequency ω are related by the linear dispersion relation. The angle between the interacting components is θ.

We now consider the form of these kernels for the water depth at Draupner of 70m. The behaviour of the sum term is comparatively straightforward. For any two interacting waves, this will be a maximum when they are travelling in the same direction (unless the ratio of the frequencies is large, in which case the assumption under which these equations are derived is invalid). Figure 4 (a) shows the variation in κ^+ for the interactions with the first peak in the Draupner spectrum. It can be seen that the sum kernel goes to zero at around 80° for all frequency interactions and is negative for angles greater than this. For the difference term the behaviour is more complex. For waves travelling in the same direction, the kernel is always non-positive. However, if the waves are travelling at widely differing angles then the kernel is positive, the value at which the kernel is zero being strongly dependent on the frequencies of the waves interacting. This is shown in Figure 4 (b).

(a) Second order sum waves

We can see evidence of second order sum waves in Figure 3. Three peaks can be seen at approximately twice the frequency of peak 1 (0.125Hz), twice the frequency of the peak 2 (0.175Hz), and the sum of the frequencies of the two peaks (0.15Hz). Unfortunately, the poor frequency resolution limits our confidence in these assertions. It should also be noted that some linear waves will be in this part of the spectrum. The relative magnitude of these three second order peaks is interesting. The peak at 0.125Hz is much larger than one at 0.175Hz. This is to be expected as peak 1 is larger than peak 2. However, the peak at 0.15Hz is substantially smaller again. This is unexpected if the wave energy from both peaks is travelling in the same direction. However, consideration of Figure 4 (a)
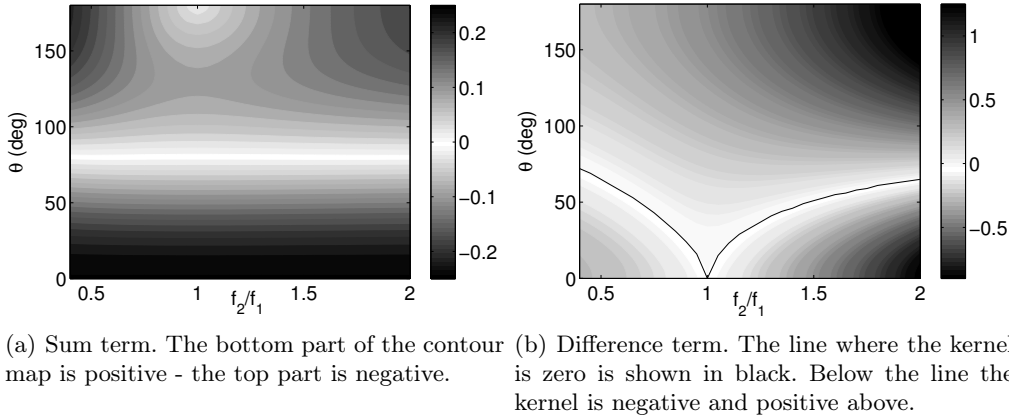
(a) Sum term. The bottom part of the contour map is positive - the top part is negative.

(b) Difference term. The line where the kernel is zero is shown in black. Below the line the kernel is negative and positive above.

Figure 4. The kernels for the second order interaction. $f_1 = 0.06$Hz and $d = 70$m.

suggests this would be expected if some of the energy in the peak 2 was travelling at an angle between perhaps 60° and 150° to the mean wave direction of peak 1.

Thus, the second order sum term is consistent with a hypothesis that a substantial portion of the wave energy in peak 2 is travelling at a large angle to the waves in peak 1. We cannot go further than this when considering the sum term due to the amount of linear information in the spectrum at these frequencies, the modification to the spectrum due to third order effects (Janssen, 2009), and the poor resolution of the Fourier transform.

(b) Second order difference waves

Adcock & Taylor (2009a) developed an approach for estimating the spreading of a sea-state from the second order difference record. As noted in section 2, they found the whole storm to have a standard deviation of spreading of 20°. However, their analysis did not work for a short section of time around the giant wave as described below.

The low frequency waves which are present in the time-history may be extracted by filtering in the frequency domain. These are shown in Figure 5, where the original time-series has been low-pass filtered at 0.03Hz. It can be seen that under the giant wave the low-pass filtered waves are positive, i.e. there is a set-up. It is not expected that any significant free waves will be propagating at frequencies this low. Therefore, the waves propagating in this part of the spectrum may be predictable from the linear waves using the interaction kernel given by equation 4.5. This predicts that energetic wave-groups in following seas will cause a set-down (Forristall, 2000). It is therefore surprising that there is a significant set-up under the giant wave in the Draupner record as noted in Walker *et al.* (2005). A set-down is observed under all other sizable wave-groups throughout the rest of the data set. One possibility is that third-order (Madsen & Fuhrman, 2006), or higher order interactions cause this set-up. To investigate this possibility we have carried out fully non-linear simulations of the Draupner wave in section 5, and find that the low frequency waves, even for a wave system up to breaking,
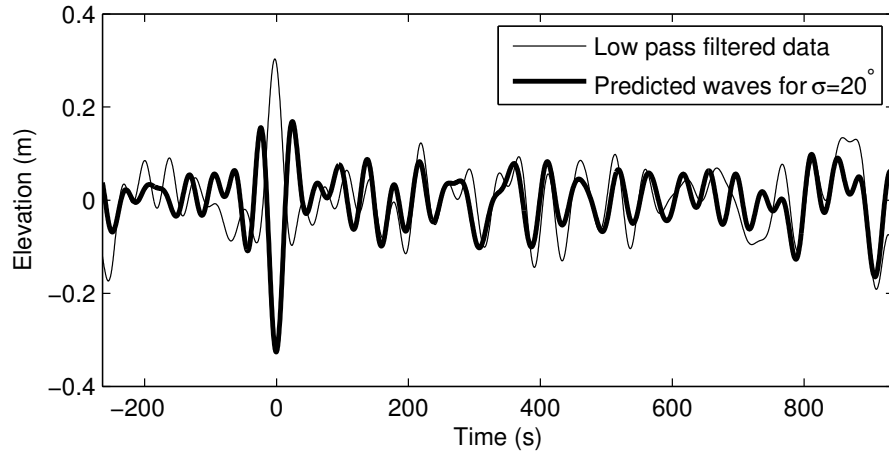
Figure 5. The low pass filtered (0.0292Hz) data for the time-history containing the New Year Wave, together with the estimate of the long waves based on a wrapped normal spreading distribution with $\sigma = 20°$.

have a set-down in the following sea, as predicted by the second order theory. Therefore, the higher order nonlinearity is not the key factor leading to the set-up in the Draupner wave.

Walker *et al.* (2005) introduced an approach to linearising a free surface time history so as to estimate the freely propagating, or linear, waves. These may then be used to estimate the low frequency waves for given spreading as set out in Adcock & Taylor (2009a). Using this linearised data, we can use a model for spreading to predict the low frequency second order difference waves. If we use a frequency independent wrapped normal spreading function

$$D\left(\theta\right) = \frac{1}{\sigma\sqrt{2\pi}}\text{Exp}\left(-\left(\frac{(\theta - \theta_0)^2}{2\sigma^2}\right)\right) \tag{4.6}$$

with σ, the standard deviation of spreading around the mean direction θ_0, of 20°, then our estimate for the low-frequency wave is as shown in Figure 5. This is clearly completely out of phase for around two minutes near the giant wave.

This suggests that either there is unusual physics happening around the giant wave, or that our model of spreading is wrong. As pointed out by Toffoli *et al.* (2007) and shown in (Figure 4 (b)), the interaction kernel can be positive if the two interacting components are propagating in different directions with a large separation angle ($> 80°$). Thus, if there are two crossing wave systems in the New Year Wave record, a set-up could occur. The remainder of this section examines this possibility.

The spectrum of the wave record for the section where the long waves are unusual is shown in Figure 6. This is 120 seconds before through to 75 seconds after the crest of the giant wave – note that this is a slightly different section of data to that used in Figure 3. Shown also in Figure 6 is the JONSWAP spectrum obtained by fitting the data excluding the period around the giant wave. We
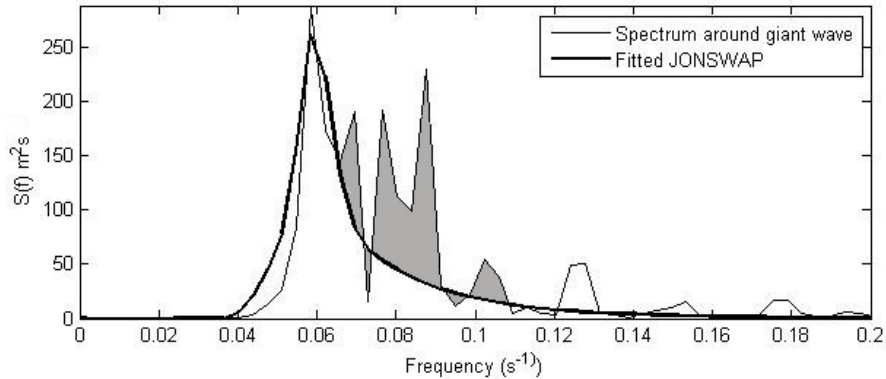
Figure 6. The spectrum around the giant wave for which the long waves are unusual. Also shown is a JONSWAP spectrum with parameters fitted to the time-series excluding this data.

now assume that the linear waves are the sum of two systems of waves: one has a JONSWAP spectrum whilst the other has a spectrum given by the difference between the actual measured spectrum and JONSWAP spectrum (the area shaded in Figure 6). We call these the 'JONSWAP waves' (J) and 'transverse waves' (t) respectively.

We have freedom to choose the phase of the individual Fourier components in the transverse wave. We can iterate these so as to try and recreate the difference wave observed in the original data. This iteration was carried out manually using the following assumptions

1. The sum of the main wave train and the transverse wave group equals the original linearised time-series.

2. The main wave train has a JONSWAP spectrum.

3. For estimating the spreading, it was assumed that both sets of waves had a spread of $20°$ about their mean value. The angle between the mean direction of the two systems of waves was ζ.

Figure 7a shows the transverse wave which produces the difference waves shown in Figure 8 when the angle between the mean direction of the wave-trains is $120°$. The main wavetrain is shown in Figure 7b. There is good agreement for around 60 seconds either side of the giant wave, regardless of exactly where the data is low-pass filtered. The sensitivity of this may be examined by varying the parameters used. In Figure 9a we vary the angle (ζ) between the mean directions of the wave-groups, in Figure 9b we vary the spreading of the transverse wave packet, in Figure 9c we vary the amplitude of the transverse waves and in Figure 9d we shift the phase of the transverse waves by $\pm 20°$.

The phasing of the transverse wave is plainly very important to recreating a difference wave similar to that observed. There is less sensitivity to changes in the other parameters. There are other wave-groups, with different phasing or frequency content, which we could use as the transverse wave-group and which would give approximately correct second order difference waves. However, we are
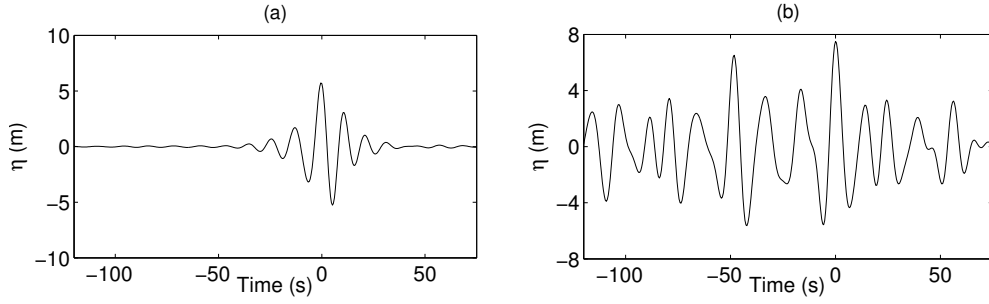
Figure 7. The combination of transverse (a) waves and JONSWAP (b) waves which produces a good fit to the observed difference terms.
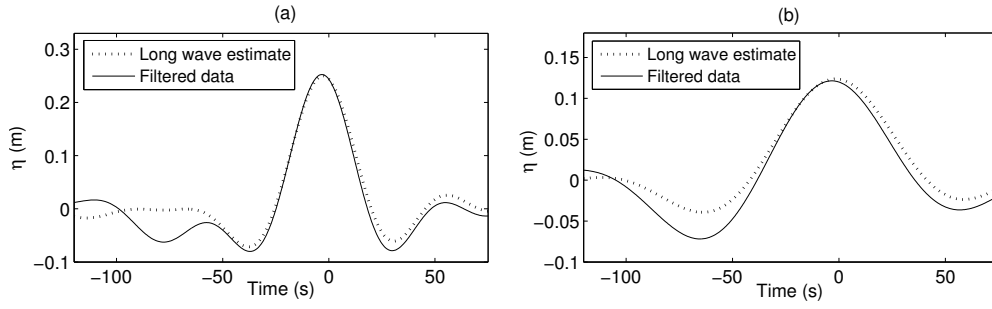

Figure 8. The difference waves under the Draupner giant wave. Comparison of filtered data and predicted second order difference waves. (a) Filtered at 0.0259Hz (b) Filtered at 0.0146Hz
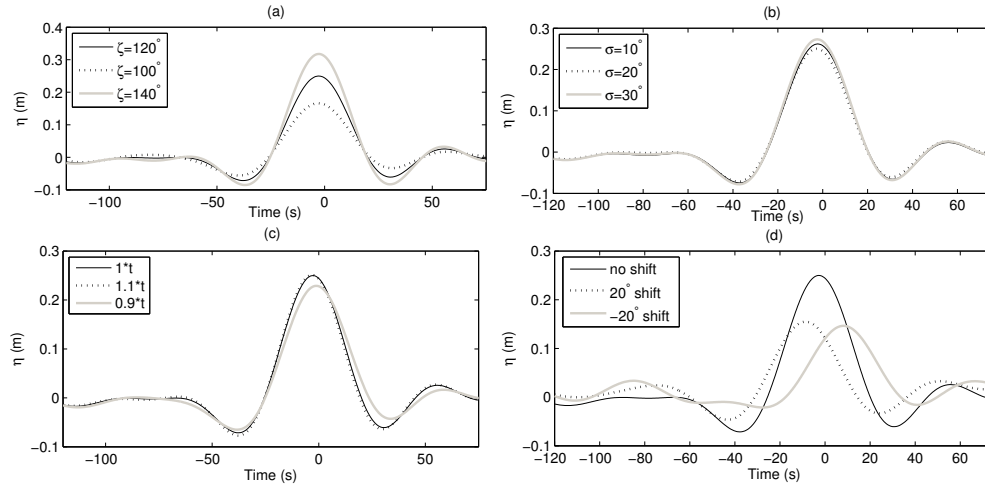

Figure 9. Sensitivity study to show how changing the parameters of the transverse wave affects the second order difference waves. (a) considers the angle between the mean wave directions. (b) varies the spreading of the transverse waves. (c) varies the amplitude of the transverse wave. (d) introduces a phase shift into all the components of the transverse wave.

certain that any such group must be propagating at an angle greater than 90° to the JONSWAP waves for the predicted long wave components to be as observed under the giant wave.

Given the lack of confidence in the sea-state details at the time of the giant crest, we have not attempted to estimate the probability of a 8m crest moving in one direction colliding with a 6m crest in a second wave group moving at close to 90°.

5. Numerical modeling of the Draupner wave

To further confirm the conclusion obtained in the above section, we have modelled the Draupner wave numerically using a fully non-linear QALE-FEM potential-flow solver. In the QALE-FEM method, the flow is governed by the fully nonlinear potential theory, where a boundary value problem for velocity potential is solved using the FEM. The main features of the QALE-FEM are that the unstructured mesh is moving at every time step using a specially developed spring analogy method for free surface problems and the velocity is calculated by a three-point technique suitable for any mesh structures (Ma, 2008; Ma & Yan, 2009; Yan & Ma, 2010a). More importantly, the QALE-FEM can model highly non-linear free surfaces and 3D overturning waves. The QALE-FEM method has been compared with experimental data and other numerical for wave breaking cases and found to be accurate (Yan & Ma, 2009, 2010b).

In all cases presented in this section we use a water depth of 70m. Average spatial discretization across the domain is 2.5m, which reduced to ~ 0.8m around the crest of the giant wave. This compares to a wavelength of ~ 230m.

(a) Modeling the Draupner wave as a wave in a following sea

We start by assuming that the Draupner wave occurred in a following sea state. To do this we use an rms spreading of 20° consistent with values discussed in section 2. We take as our initial conditions a NewWave (Boccotti, 1983; Tromans *et al.*, 1991) which would have a linear amplitude (when focused) of 14.7m (as estimated by Walker *et al.* (2005) for the Draupner wave) and use the 'linearised' spectrum (Walker *et al.*, 2005; Adcock & Taylor, 2009a) for a ten minute record around the giant wave. When the higher order harmonics are added Walker *et al.* found this reproduced the measured free surface with the anomalous set-up filtered out. We then run the linear profile back in time for 100 seconds assuming linear evolution and use this as the initial conditions for the non-linear simulation, after correcting the free surface and velocity potential using second order theory.

The numerical simulations have been carried out for a number of cases by gradually increasing the amplitude until the wave overturning occurs as shown in Figure 11. Various mesh sizes were used to ensure that these results were robust. Our simulation for the largest non-breaking wave has a time-history similar to that measured at Draupner as shown in Figure 10, in which both time-histories have had the low-frequency components removed, and the signals match well around the large peak although the amplitude of the main crest is slightly too small. However, any increase in amplitude or steepness over this results in wave overturning. This result is consistent with the physical wave-tank experiments
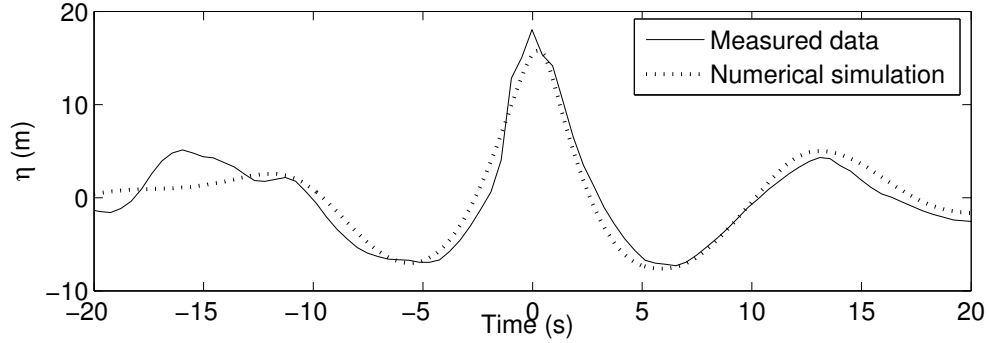
Figure 10. Free surface profile (high pass filtered at 0.038Hz) showing a comparison of the numerical simulation for the following sea case with the recorded data.
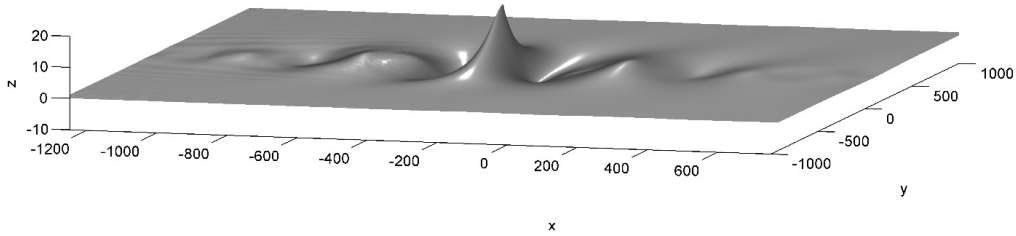

Figure 11. A wave-group on the point of breaking, when we try to recreate a wave with the amplitude of the Draupner wave in a following sea.

of Clauss & Klein (2009), whose attempt to reproduce the Draupner wave uni-directionally resulted in a scaled crest height slightly smaller than that measured. They found that this wave was on the point of breaking

After low-pass filtering the simulation in Figure 10, we see the expected set-down, shown in Figure 12 together with the second-order theoretical result based on a linearised profile and a spreading of 20° (although the actual spreading will be slightly smaller than this due to the non-linear changes to the group shape (Gibbs & Taylor, 2005; Adcock, 2009). The figure confirms that, whilst there is a small mismatch, the second order theory is clearly still applicable in this case. More importantly, this figure implies that in the following sea state, the long wave (or the difference wave) components produce a set-down beneath an energetic group rather than set-up.

(b) Modeling the Draupner wave as a wave in a crossing sea

We have also carried out fully non-linear modelling of the two wave-groups which are crossing in order to look at if the set-up can appear as predicted by the second order theory in Section 4. We assume that each wave-group has a NewWave type profile and that the two mean wave directions are separated by
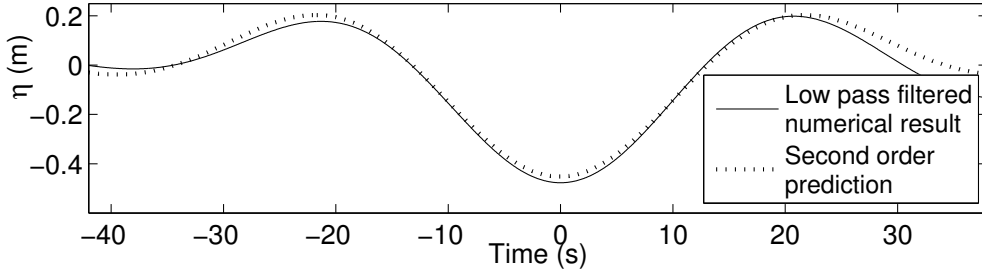
Figure 12. Numerical data low pass filtered at 0.035Hz from numerical simulations for a following sea. Time is set to zero under the giant wave. Also shown is the predicted difference wave based on second order theory.
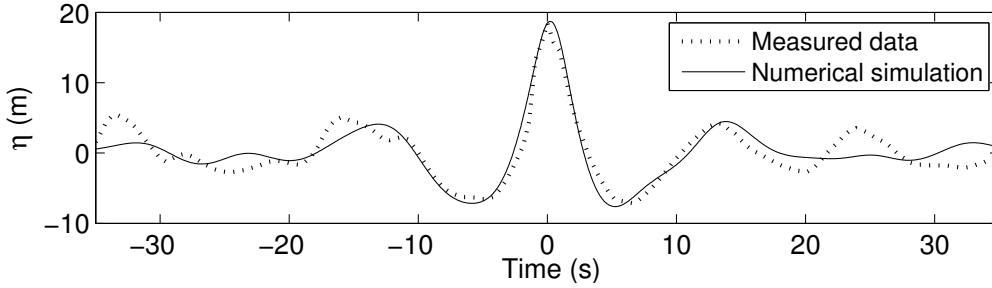

Figure 13. Free surface profile showing the comparison of the numerical simulation for the crossing sea case with the recorded data.

$120°$ and that each group has an r.m.s. spreading about its mean direction of $20°$. We start our simulations 60 seconds before linear focus, but in this case we have modified the initial conditions so that both groups focus at the same spatial point. In the crossing sea case, the waves with different amplitudes have also been investigated and shown that they do not break, even for the cases higher and steeper than the Draupner wave. The case with a profile very close to that of the Draupner wave is shown in Figure 13, where the crest of the numerical results is very close to the crest of the field measured data (18.7m). The corresponding low-pass filtered time history of the simulation (at 0.034Hz) is given in Figure 14, together with the low-pass filtered data of the Draupner wave. Although there is inevitably some difference between them due to lack of information in the field data, this comparison shows that in the crossing wave case, the fully nonlinear simulation leads to local long wave set-up, again confirming the prediction of the second order theory discussed in Section 4.

6. Discussion of analytical and numerical results

In sections 4 and 5 we have investigated the causes of the low frequency set-up under the Draupner wave. The numerical modelling demonstrates that for very steep, moderately broadbanded, waves, second order theory gives a good model
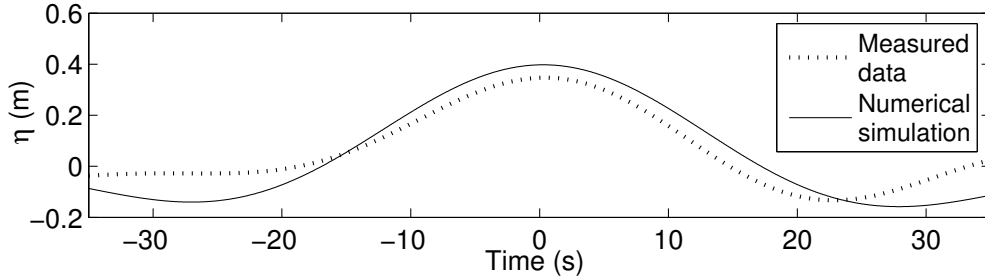
Figure 14. Comparison of long waves in the crossing sea numerical simulation and the low pass filtered Draupner data.

for the long waves in a record. Thus we can conclude that a "set-up" will only occur under a large wave if its energy is not confined to a narrow directional spectrum.

Some discussion needs to be made as to the assumptions we have used in the reconstruction of the wave. Various alternative scenarios could be imagined where, consistent with second order theory, a set-up results. However, given the evidence of the ECMWF hindcast, the most probable scenario is the wave was caused by two wave-packets colliding whose mean wave directions were separated by more than 90°. We cannot, of course, be accurate in giving this angle exactly, or in reconstructing the distribution of energy between the two wave-packets.

Finally, we remark on our choice of spreading function for the two wave systems. We have used a simple frequency-independent Gaussian form. Other more complex choices are possible, a well-validated frequency-dependent model is given by Ewans (1998). However, our predictions of set-up/set-down for the Draupner wave only work when the two wave trains are separated by more than 90°, well beyond the range of spreading consistent with the Ewans' form. Almost any reasonable choice for the spreading forms for the two individual trains will give comparable results for the set-up only if they are separated in mean direction by at least 90°.

7. Forces on the structure

The forces due to this wave on the northern platform of the two at the Draupner field were significantly lower than would have been expected for a wave of this size (Haver, 2004; Hansteen *et al.*, 2003). Given that the height of the Draupner wave is roughly the 50-100 year design condition for that part of the North Sea, the observed peak horizontal force on the structure, as recorded by strain gauges on the suction caisson foundations and lower structural members, was roughly half of that expected for a wave of this height.

If the two wave components of amplitudes 8 and 6m were travelling at close to 90° apart in direction, but in phase locally in time, the net horizontal velocity amplitude would be approximately proportional to vector $(8, 6)$, resulting in a combined velocity equivalent to a 10m wave since $10 = \sqrt{8^2 + 6^2}$. In contrast, if the wave system were close to collinear, the vector sum would be $(14, 0)$. Taking

the Morison drag as proportional to velocity magnitude squared, this gives a peak force proportional to 10^2 for the crossing system, compared to 14^2 had the wave been collinear. Hence, we suspect that the unexpectedly low value of the total horizontal load on the structure, as observed by Hansteen *et al.* (2003), is at least consistent with the giant wave arising in a crossing sea-state.

8. Other freak wave events in crossing seas

Most studies of freak waves investigate the dynamics of extreme waves in following seas (see reviews Kharif & Pelinovsky (2003); Dysthe *et al.* (2008)). This is because non-linear Benjamin-Feir type instabilities only occur in seas which have a small directional spreading (Waseda *et al.*, 2009). Recent studies by Onorato *et al.* (2006*b*); Shukla *et al.* (2007) have looked at the non-linear dynamics of wave-groups in crossing seas, and Donelan & Magnusson (2005) looked at the statistics of waves in such seas, but at present the understanding of these sea-states has not been as thoroughly researched as that for following seas.

However, as well as the evidence presented in this paper, there is other evidence that unusual and dangerous waves do occur in crossing seas. Ferreira de Pinho *et al.* (2004) studied extreme waves in the Campos basin off Brazil. They only observed extreme waves ($H/H_s > 2.4$) in sea-states which were highly directionally spread and can be assumed to be crossing seas. Rosenthal & Lehner (2008) also found evidence that freak waves occur in crossing sea-states.

Toffoli *et al.* (2005) studied the sea-states in which maritime accidents are known to have occurred. They found a very high proportion of these occurred in crossing seas as two systems of waves merged. This is unsurprising since crossing seas are notoriously difficult for ships to navigate through. However, what was surprising is the number of accidents which occurred when the swell was much smaller (less than 20% as energetic) than the wind sea, the situation our analysis suggests was the case at Draupner.

There are a number of anecdotal accounts of extreme waves having unusual directional properties. An account in a BBC Horizon programme of an unusual wave hitting the cruise ship Caledonian Star in 2001 states that this wave was travelling at $30°$ to the waves around it. Video recorded during filming for *The Deadliest Catch* apparently shows a fishing boat being hit broadside by a large wave travelling at around $90°$ to the main wave system. The giant wave which hit the Queen Mary in 1942 is described as hitting her 'broadside', so presumably this wave was travelling at roughly $90°$ to the majority of the waves. Similar accounts are given by the crews of the Gloucester dragger (Prybot, 2007) and the RMS Etruria (Liu, 2007).

9. Conclusions

The Draupner wave was an event which was extremely improbable in a standard second order model of the sea-state. There is no obvious physical reason why the amplitude of the wave should be larger than that expected in a model based on linear wave-group evolution. Certainly Benjamin-Feir type instabilities, as

we currently understand these, would not cause this wave as these would be suppressed by the finite depth and the directional spreading of the sea-state.

The Draupner wave has an unusual feature, that is the long wave (or low frequency wave) components give a set-up under the giant wave. In this paper, we first apply second order theory to show that the set-up of the long waves was the result of two wave-packets whose mean wave direction was separated by around 90° or more. This explanation is consistent with all the other evidence the authors have been able to find. These include the hindcast of the sea-state and the measured forces on the structure. Secondly, we carry out fully nonlinear numerical modelling. This confirms that the set-up cannot occur in the following sea but would occur in a crossing sea. This modelling also shows that a wave as steep as the Draupner wave would break in a following sea, whereas it would not in a crossing sea. Therefore, our investigations in this paper lead to the conclusion that the set-up of the long wave components, and hence the giant Draupner wave, is the result of the two wave groups propagating at a large angle.

This paper does not explain why the wave was so large (although the set-up, as opposed to a set-down, does add 1m to the crest elevation above mean sea level). However, we discuss other evidence that freak waves do occur in crossing sea-states, suggesting that there may be some physical process which occurs as two wave systems merge which causes abnormal waves.

Acknowledgment

References

Adcock, T. A. A. 2009 Aspects of wave dynamics and statistics on the open ocean. DPhil Thesis, University of Oxford.

Adcock, T. A. A. & Taylor, P. H. 2009a Estimating ocean wave directional spreading from an Eulerian surface elevation time-history. *Proc. Roy. Soc. A*, **465**(2111), 3361–3381. (doi:10.1098/rspa.2009.0031)

Adcock, T. A. A. & Taylor, P. H. 2009b Focusing of unidirectional wave-groups on deep water, an approximate NLS-equation based model. *Proc. Roy. Soc. A*, **465**(2110), 3083–3102. (doi:10.1098/rspa.2009.0224)

Adcock, T. A. A. & Yan, S. 2010 The focusing of uni-directional Gaussian wave-groups in finite depth. In *Proc. 29th Int. Conf. Ocean, Offshore and Arctic Engineering (OMAE), Shanghai, China*, p. 20993.

Boccotti, P. 1983 Some new results on statistical properties of wind waves. *Appl. Ocean Res.*, **5**, 134–140.

Christou, M., Tromans, P., Vanderschuren, L. & Ewans, K. 2009 Second-Order Crest Statistics Of Realistic Sea States. In *Proceedings of the 11th International Workshop on Wave Hindcasting and Forecasting, Halifax, Canada.*

Clauss, G. F. & Klein, M. 2009 The New Year Wave: Spatial Evolution of an Extreme Sea State. *Journal of Offshore Mechanics and Arctic Engineering*, **131**(4), 041001. (doi:10.1115/1.3160533)

Dalzell, J. F. 1999 A note on finite depth second-order wave-wave interactions. *Applied Ocean Research*, **21**(3), 105–111. (doi:10.1016/S0141-1187(99)00008-5)

Dean, R. G. & Sharma, J. N. 1981 Simulation of Wave Systems due to Non-Linear Directional Spectra. In *Proceedings, International Symposium on Hydrodynamics in Ocean Engineering*, vol. 2, pp. 1211–1222. Norwegian Institute of Technology, Trondheim, Norway.

Donelan, M. A. & Magnusson, A. K. 2005 The role of meteorological focusing in generating rogue wave conditions. In *Proceedings of the 14th winter workshop 'Aha Huliko'.*

Dysthe, K., Krogstad, H. E. & Muller, P. 2008 Oceanic rogue waves. *Annual Review of Fluid Mechanics*, **40**(1), 287–310. (doi:10.1146/annurev.fluid.40.111406.102203)

Ewans, K. C. 1998 Observations of the directional spectrum of fetch-limited waves. *J. Phys. Oceanogr.*, **28**, 495–512.

Ewans, K. C. & Buchner, B. 2008 Wavelet analysis of an extreme wave in a model basin. In *Proc. 27 Int. Conf. Offshore Mech and Arctic Engg., Estoril, Portugal.* 57499.

Ferreira de Pinho, U., Liu, P. C. & Ribeiro, C. E. P. 2004 Freak Waves at Campos Basin, Brazil. *Geofizica*, **22**, 53–67.

Forristall, G. Z. 2000 Wave crest distributions: Observations and second-order theory. *J. Phys. Oceanogr.*, **30**, 1931Ű–1943. (doi:10.1175/1520-0485(2000) 030<1931:WCDOAS>2.0.CO;2)

Gibbs, R. G. & Taylor, P. H. 2005 Formation of walls of water in ŚfullyŠ nonlinear simulations. *Applied Ocean Research*, **27**(3), 142–157. (doi:10.1016/j.apor.2005.11.009)

Gramstad, O. & Trulsen, K. 2007 Influence of crest and group length on the occurrence of freak waves. *Journal of Fluid Mechanics*, **582**(1), 463 – 472. (doi:10.1017/S0022112007006507)

Guedes Soares, C., Cherneva, Z. & Antão, E. M. 2004 Steepness and asymmetry of the largest waves in storm sea states. *Ocean Engineering*, **31**(8-9), 1147 – 1167. (doi:10.1016/j.oceaneng.2003.10.014)

Hansteen, O. E., Jostad, H. P. & Tjelta, T. I. 2003 Observed platform response to a "monster" wave. In *Field measurements in geomechanics*, pp. 73–86. Sweets & Zeitlinger.

Haver, S. 2004 A Possible Freak Wave Event Measured at the Draupner Jacket January 1 1995. In *Rogue waves Workshop, Brest. www.ifremer.fr/web-com/stw2004/rw/fullpapers/walk_ on_ haver.pdf.*

Hjelmervik, K. B. & Trulsen, K. 2009 Freak wave statistics on collinear currents. *J. Fluid Mech.*, **637**, 267–284. (doi:10.1017/S0022112009990607)

Janssen, P. A. E. M. 2003 Nonlinear Four-Wave Interactions and Freak Waves. *J. Phys. Oceanogr.*, **33**, 863–884.

Janssen, P. A. E. M. 2009 On some consequences of the canonical transformation in the Hamiltonian theory of water waves. *Journal of Fluid Mechanics*, **637**(1), 1–44. (doi:10.1017/S0022112009008131)

Janssen, P. A. E. M. & Onorato, M. 2007 The Intermediate Water Depth Limit of the Zakharov Equation and Consequences for Wave Prediction. *J. Phys. Oceanogr.*, **37**, 2389–2400.

Jensen, J. J. 2005 Conditional second-order short-crested water waves applied to extreme wave episodes. *J. Fluid Mech.*, **545**, 29–40. (doi:10.1017/S0022112005006841)

Jensen, R. E., Cardone, V. J. & Cox, A. T. 2006 Performance of third generation wave models in extreme hurricanes. In *9th International Wind and Wave Workshop, September 25-29, Victoria, BC.*

Johannessen, T. B. & Swan, C. 2001 A laboratory study of the focusing of transient and directionally spread surface water waves. *Proc. R. Soc. A*, **457**, 971–1006. (doi:10.1017/S0022112005006841)

Katsardi, V. & Swan, C. 2011 The evolution of large non-breaking wave in intermediate and shallow water. I. Numerical calculations of uni-directional seas. *Proc. R. Soc. A*, **467**(2127), 778–805. (doi:10.1098/rspa.2010.0280)

Kharif, C. & Pelinovsky, E. 2003 Physical mechanisms of the rogue wave phenomenon. *European Journal of Mechanics - B/Fluids*, **22**(6), 603–634. (doi:10.1016/j.euromechflu.2003.09.002)

Komen, G. J., Cavaleri, L., Donelan, M., Hasselmann, K., Hasselmann, S. & Janssen, P. A. E. M. 1994 *Dynamics and modelling of ocean waves.* CUP.

Krogstad, H. E., Magnusson, A.-K. & Donelan, M. A. 2006 Wavelet and Local Directional Analysis of Ocean Waves. *Int. J. Offshore and Polar Eng.*, **16**, 97–103.

Liu, P. C. 2007 A chronology of freaque wave encounters. *Geofizika*, **24**(1), 57–70.

Ma, Q. W. 2008 Numerical Generation of Freak Waves Using MLPG_R and QALE-FEM Methods. *CMES*, **18**, 223–234. (doi:10.1016/j.jcp.2005.06.014)

Ma, Q. W. & Yan, S. 2009 QALE-FEM for Numerical Modelling of Nonlinear Interaction between 3D Moored Floating Bodies and Steep Waves. *International Journal for Numerical Methods in Engineering*, **78**, 713–756. (doi:10.1016/j.jcp.2005.06.014)

Madsen, P. A. & Fuhrman, D. R. 2006 Third-order theory for bichromatic bi-directional water waves. *J.Fluid Mech.*, **557**, 369–397. (doi:10.1017/S0022112006009815)

Onorato, M., Osborne, A., Serio, M., Cavaleri, L., Brandini, C. & Stansberg, C. 2006*a* Extreme waves, modulational instability and second order theory: wave flume experiments on irregular waves. *European Journal of Mechanics - B/Fluids*, **25**(5), 586–601. (doi:10.1016/j.euromechflu.2006.01.002)

Onorato, M., Osborne, A. R. & Serio, M. 2006*b* Modulational Instability in Crossing Sea States: A Possible Mechanism for the Formation of Freak Waves. *Phys. Rev. Lett.*, **96**(1), 014 503.

Onorato, M., Waseda, T., Toffoli, A., Cavaleri, L., Gramstad, O., Janssen, P. A. E. M., Kinoshita, T., Monbaliu, J., Mori, N. *et al.* 2009 Statistical properties of directional ocean waves: The role of the modulational instability in the formation of extreme events. *Physical Review Letters*, **102**(11), 114502. (doi:10.1103/PhysRevLett.102.114502)

Prybot, P. K. 2007 Rogue wave slams Gloucester dragger. Gloucester Daily Times, 28 April 2007.

Rosenthal, W. & Lehner, S. 2008 Rogue Waves: Results of the MaxWave Project. *Journal of Offshore Mechanics and Arctic Engineering*, **130**(2). (doi:10.1115/1.2918126)

Shukla, P. K., Marklund, M. & Stenflo, L. 2007 Modulational instability of nonlinearly interacting incoherent sea states. *JETP Letters*, **84**(12). (doi:10.1134/S0021364006240039)

Toffoli, A., Gramstad, O., Trulsen, K., Monbaliu, J., Bitner-Gregersen, E. & Onorato, M. 2010 Evolution of weakly nonlinear random directonal wave: laboratory experiments and numerical simulations. *J. Fluid Mech.*, **664**, 313–336. (doi:10.1017/S002211201000385X)

Toffoli, A., Lefèvre, J., Bitner-Gregersen, E. & Monbaliu, J. 2005 Towards the identification of warning criteria: Analysis of a ship accident database. *Applied Ocean Research*, **27**(6), 281 – 291. (doi:10.1016/j.apor.2006.03.003)

Toffoli, A., Onorato, M., Babanin, A., Bitner-Gregersen, E., Osborne, A. & Monbaliu, J. 2007 Second-Order Theory and Setup in Surface Gravity Waves: A Comparison with Experimental Data. *J. Phys. Oceanogr.*, **37**, 2726Ũ–2739. (doi:10.1175\%2F2007JPO3634.1 N2)

Tromans, P. S., Anaturk, A. & Hagemeijer, P. 1991 A new model for the kinematics of large ocean waves– application as a design wave. In *Proc. 1st Int. Conf. Offshore Mech. and Polar Engng (ISOPE)*, vol. 3, pp. 64–71.

Trulsen, K. 2001 Simulating the spatial evolution of a measured time series of a freak wave. In *Proceedings of rogue waves 2000*, pp. 265–273.

Walker, D. A. G., Taylor, P. H. & Eatock Taylor, R. 2005 The shape of large surface waves on the open sea and the Draupner New Year wave. *Applied Ocean Research*, **26**(3-4), 73–83. (doi:10.1016/j.apor.2005.02.001)

Waseda, T., Kinoshita, T. & Tamura, H. 2009 Interplay of resonant and quasi-resonant interaction of the directional ocean waves. *J. Phys. Oceanogr.*, **39**, 2351–2362. (doi:10.1175/2009JPO4147.1)

Yan, S. & Ma, Q. W. 2009 Nonlinear Simulations of 3D Freak Waves Using a Fast Numerical Method. *International Journal of Offshore and Polar Engineering*, **19**(3), 168–175.

Yan, S. & Ma, Q. W. 2010*a* Numerical Simulation of Interaction between Wind and 2-D Freak Waves. *European Journal of Mechanics - B/Fluids*, **29**(1), 18–31.

Yan, S. & Ma, Q. W. 2010*b* QALE-FEM for modelling 3D overturning waves. *International Journal for Numerical Methods in Fluids*, **63**, 743–768. (doi: 10.1002/fld.2100)

Zheng, X. Y. & Moan, T. 2010 Freak Waves Within The Third Order Model. In *Proc. 29th Int. Conf. Ocean, Offshore and Arctic Engineering (OMAE), Shanghai, China*, p. 20455.